2014

Measurement of "Pretzelosity" Asymmetry of Charged Pion Production in Semi-Inclusive Deep Inelastic Scattering on a Polarized ^{3}He Target

Y. Zhang

X. Qian

K. Allada

C. Dutta

M. Canan
Old Dominion University

See next page for additional authors

Original Publication Citation

Zhang, Y., Qian, X., Allada, K., Dutta, C., Huang, J., Katich, J., . . . Jefferson Lab Hall, A. C. (2014). Measurement of "pretzelosity" asymmetry of charged pion production in semi-inclusive deep inelastic scattering on a polarized ^{3}He target. *Physical Review C, 90*(5), 055209. doi:10.1103/PhysRevC.90.055209

Measurement of "pretzelosity" asymmetry of charged pion production in semi-inclusive deep inelastic scattering on a polarized ^{3}He target

Y. Zhang,[1,*] X. Qian,[2,3] K. Allada,[4,5] C. Dutta,[4] J. Huang,[5,6] J. Katich,[7] Y. Wang,[8] K. Aniol,[9]
J. R. M. Annand,[10] T. Averett,[7] F. Benmokhtar,[11] W. Bertozzi,[5] P. C. Bradshaw,[7]
P. Bosted,[12] A. Camsonne,[12] M. Canan,[13] G. D. Cates,[14] C. Chen,[15] J.-P. Chen,[12]
W. Chen,[2] K. Chirapatpimol,[14] E. Chudakov,[12] E. Cisbani,[16,17] J. C. Cornejo,[9] F. Cusanno,[16,17]
M. M. Dalton,[14] W. Deconinck,[5] C. W. de Jager,[12,14] R. De Leo,[18] X. Deng,[14]
A. Deur,[12] H. Ding,[14] P. A. M. Dolph,[14] D. Dutta,[19] L. El Fassi,[20] S. Frullani,[16,17]
H. Gao,[2] F. Garibaldi,[16,17] D. Gaskell,[12] S. Gilad,[5] R. Gilman,[12,20] O. Glamazdin,[21]
S. Golge,[13] L. Guo,[6] D. Hamilton,[10] O. Hansen,[12] D. W. Higinbotham,[12] T. Holmstrom,[22]
M. Huang,[2] H. F. Ibrahim,[23] M. Iodice,[24] X. Jiang,[20,6] G. Jin,[14] M. K. Jones,[12]
A. Kelleher,[7] W. Kim,[25] A. Kolarkar,[4] W. Korsch,[4] J. J. LeRose,[12] X. Li,[26] Y. Li,[26]
R. Lindgren,[14] N. Liyanage,[14] E. Long,[27] H.-J. Lu,[28] D. J. Margaziotis,[9] P. Markowitz,[29]
S. Marrone,[18] D. McNulty,[30] Z.-E. Meziani,[31] R. Michaels,[12] B. Moffit,[5,12] C. Muñoz Camacho,[32]
S. Nanda,[12] A. Narayan,[19] V. Nelyubin,[14] B. Norum,[14] Y. Oh,[33] M. Osipenko,[34]
D. Parno,[11,35] J. C. Peng,[8] S. K. Phillips,[27] M. Posik,[31] A. J. R. Puckett,[5,6] Y. Qiang,[2,12] A. Rakhman,[36] R. D. Ransome,[20]
S. Riordan,[14] A. Saha,[12,†] B. Sawatzky,[31,12] E. Schulte,[20] A. Shahinyan,[37] M. H. Shabestari,[14,19] S. Širca,[38] S. Stepanyan,[25]
R. Subedi,[14] V. Sulkosky,[5,12] L.-G. Tang,[15] W. A. Tobias,[14] G. M. Urciuoli,[16] I. Vilardi,[18] K. Wang,[14] B. Wojtsekhowski,[12]
X. Yan,[28] H. Yao,[31] Y. Ye,[28] Z. Ye,[15] L. Yuan,[15] X. Zhan,[5] Y.-W. Zhang,[1] B. Zhao,[7] X. Zheng,[14]
L. Zhu,[8,15] X. Zhu,[2] and X. Zong[2]
(Jefferson Lab Hall A Collaboration)

[1]*Lanzhou University, Lanzhou 730000, Gansu, People's Republic of China*
[2]*Duke University, Durham, North Carolina 27708, USA*
[3]*Physics Department, Brookhaven National Laboratory, Upton, New York 11973, USA*
[4]*University of Kentucky, Lexington, Kentucky 40506, USA*
[5]*Massachusetts Institute of Technology, Cambridge, Massachusetts 02139, USA*
[6]*Los Alamos National Laboratory, Los Alamos, New Mexico 87545, USA*
[7]*College of William and Mary, Williamsburg, Virginia 23187, USA*
[8]*University of Illinois, Urbana-Champaign, Illinois 61801, USA*
[9]*California State University, Los Angeles, Los Angeles, California 90032, USA*
[10]*University of Glasgow, Glasgow G12 8QQ, Scotland, United Kingdom*
[11]*Carnegie Mellon University, Pittsburgh, Pennsylvania 15213, USA*
[12]*Thomas Jefferson National Accelerator Facility, Newport News, Virginia 23606, USA*
[13]*Old Dominion University, Norfolk, Virginia 23529, USA*
[14]*University of Virginia, Charlottesville, Virginia 22904, USA*
[15]*Hampton University, Hampton, Virginia 23187, USA*
[16]*INFN, Sezione di Roma, I-00161 Rome, Italy*
[17]*Istituto Superiore di Sanità, I-00161 Rome, Italy*
[18]*INFN, Sezione di Bari and University of Bari, I-70126 Bari, Italy*
[19]*Mississippi State University, Mississippi 39762, USA*
[20]*Rutgers, The State University of New Jersey, Piscataway, New Jersey 08855, USA*
[21]*Kharkov Institute of Physics and Technology, Kharkov 61108, Ukraine*
[22]*Longwood University, Farmville, Virginia 23909, USA*
[23]*Cairo University, Giza 12613, Egypt*
[24]*INFN, Sezione di Roma3, I-00146 Rome, Italy*
[25]*Kyungpook National University, Taegu 702-701, Republic of Korea*
[26]*China Institute of Atomic Energy, Beijing, People's Republic of China*
[27]*University of New Hampshire, Durham, New Hampshire 03824, USA*
[28]*University of Science and Technology of China, Hefei 230026, People's Republic of China*
[29]*Florida International University, Miami, Florida 33199, USA*
[30]*University of Massachusetts, Amherst, Massachusetts 01003, USA*
[31]*Temple University, Philadelphia, Pennsylvania 19122, USA*
[32]*Université Blaise Pascal/IN2P3, F-63177 Aubière, France*
[33]*Seoul National University, Seoul 151-747, Republic of Korea*
[34]*INFN, Sezione di Genova, I-16146 Genova, Italy*
[35]*University of Washington, Seattle, Washington 98195, USA*
[36]*Syracuse University, Syracuse, New York 13244, USA*

[37] *Yerevan Physics Institute, Yerevan 375036, Armenia*
[38] *University of Ljubljana, SI-1000 Ljubljana, Slovenia*

(Received 12 December 2013; revised manuscript received 11 October 2014; published 24 November 2014)

An experiment to measure single-spin asymmetries of semi-inclusive production of charged pions in deep-inelastic scattering on a transversely polarized ^{3}He target was performed at Jefferson Laboratory in the kinematic region of $0.16 < x < 0.35$ and $1.4 < Q^2 < 2.7$ GeV^2. Pretzelosity asymmetries on ^{3}He, which are expressed as the convolution of the $h_{1T}^{\perp}$ transverse-momentum-dependent distribution functions and the Collins fragmentation functions in the leading order, were measured for the first time. Under the effective polarization approximation, we extracted the corresponding neutron asymmetries from the measured ^{3}He asymmetries and cross-section ratios between the proton and ^{3}He. Our results show that both $\pi^{\pm}$ on ^{3}He and on neutron pretzelosity asymmetries are consistent with zero within experimental uncertainties.

DOI: 10.1103/PhysRevC.90.055209 PACS number(s): 25.30.Fj, 24.85.+p, 25.30.Rw

I. INTRODUCTION

Studies of nucleon structure have been and still are at the frontier of understanding how quantum chromodynamics (QCD) works in the nonperturbative region. It has been known for decades that the nucleon is composed of quarks and gluons. However, how quarks and gluons contribute to the elementary properties of the nucleon is still an open question. Among these properties, the nucleon spin has been at the center of interest for more than two decades since the European Muon Collaboration's discovery that quark spins were found to contribute only a small portion to the nucleon spin [1]. In last two decades, polarized deep-inelastic scattering (DIS) experiments [2] have confirmed that the quark spin only contributes to about 25% of the nucleon spin with significantly improved precision. In more recent years, efforts have also been devoted to the determination of the gluon's intrinsic contribution to the nucleon spin both from fixed-target polarized DIS and from polarized proton-proton collision measurements [3]. New results [4–6] from the Relativistic Heavy Ion Collider spin program suggest that the gluon spin may only contribute to the proton spin at a level comparable to those of quark spins. These findings suggest that the orbital angular momentum (OAM) of quarks and gluons, the most elusive piece, may actually be the largest contributor.

In recent years, major theoretical and experimental efforts have focused on accessing the OAM of quarks. The development of the general parton distribution functions (GPDs) [7] and the transverse-momentum-dependent parton distribution functions (TMDs) [8] provides not only the three-dimensional imaging of the nucleon, but also promising ways to access OAM. By investigating correlations between the quark position and the momentum, GPDs supply a new way to characterize the contribution of the quarks' orbital motion to the spin of the nucleon. On the other hand, TMDs investigate the parton distributions in three-dimensional momentum space and provide information about the relationship between the quark momenta and the spin of either the nucleon or the quark. Most TMDs are expected to vanish in the absence of quark orbital motion. Thus they supply important and complementary (to GPDs) ways to access the OAM's contribution to the nucleon spin.

Among the eight leading-twist TMDs, there are only three that remain nonzero after integrating over the parton transverse momentum [8]. They are the unpolarized parton distribution function (PDF) f_1, the longitudinally polarized PDF g_1 (helicity), and the transversely polarized PDF h_1 (transversity). The distribution f_1 has been extensively studied for several decades. The distribution g_1 is also relatively well understood by continuous efforts since the 1970s [2]. For the h_1, although less known than the former two, pioneering studies were made in recent years, both theoretically and experimentally [9]. One of the least known TMDs, $h_{1T}^{\perp}$, referred to as pretzelosity, has drawn significant attention recently [10–14] due to its intuitive relation to the quark OAM. As one of the eight leading-twist TMDs, it has a probabilistic interpretation as in a transversely polarized nucleon the parton number density of which is transversely polarized in a direction perpendicular to the nucleon polarization direction, subtracted by the parton number density with the opposite parton-polarization direction. As with transversity, pretzelosity also has an odd chirality, which leads to an important consequence that there are only quark pretzelosity distributions, with no gluonic counterparts.

In a class of relativistic quark models [13,14], pretzelosity can be expressed as the difference between the helicity and the transversity. In the light cone the difference of quark polarization between the longitudinal and transverse direction is due to the fact that boost and rotation operators do not commute. A nonzero value of the pretzelosity is thus a direct consequence of this relativistic nature of quark motion. Another interesting feature is that pretzelosity emerges from the interference of quark wave-function components differing by two units of orbital angular momentum [15]. Pretzelosity is the only leading-twist TMD carrying this unique feature. In certain models, the quark OAM can be directly accessed via pretzelosity [13,14]. This finding was first obtained in a quark-diquark model [16] and a bag model [12], and then confirmed in a large class of quark models respecting spherical symmetry [14].

In experiments, pretzelosity is suppressed in the inclusive DIS processes due to its chiral-odd nature. However,

*Corresponding author: yizhang@lzu.edu.cn
†Deceased.

combined with another chiral-odd object such as the Collins fragmentation function [17], it leads to a measurable effect in the semi-inclusive DIS (SIDIS) [18] in which a leading hadron is detected in addition to the scattered lepton. Specifically, with an unpolarized lepton beam scattered from a transversely polarized nucleon target, a nonzero $h_{1T}^{\perp}$ would produce an azimuthal angular dependent single-spin asymmetry (SSA).

At the leading twist and following the Trento convention [19], the azimuthal angular dependence of the target SSA can be written as

$$\begin{aligned} A_{UT}(\phi_h,\phi_s) &= \frac{1}{P_{^3\mathrm{He}}}\frac{Y(\phi_h,\phi_s)-Y(\phi_h,\phi_s+\pi)}{Y(\phi_h,\phi_s)+Y(\phi_h,\phi_s+\pi)} \\ &\approx A^C\sin(\phi_h+\phi_s)+A^S\sin(\phi_h-\phi_s) \\ &\quad + A^p\sin(3\phi_h-\phi_s), \end{aligned} \tag{1}$$

where the subscripts U and T stand for the unpolarized beam and the transversely polarized target, respectively. $P_{^3\mathrm{He}}$ is the polarization of the target, Y is the normalized yield, ϕ_h is the angle between the lepton plane and the hadron plane, which is defined by the hadron momentum direction and the virtual photon momentum direction, and ϕ_s is the angle between the target spin direction and the lepton plane. The three leading-twist asymmetries [20] correspond to the Collins asymmetry (A^C), the Sivers asymmetry (A^S), and the pretzelosity asymmetry (A^p). The Collins asymmetry is the transversity distribution function convoluted with the Collins fragmentation function, while the Sivers asymmetry is the Sivers distribution function convoluted with the unpolarized fragmentation function. The last term, referred to as the pretzelosity asymmetry, is the pretzelosity distribution function convoluted with the Collins fragmentation function. As shown in Eq. (1), these three terms have different azimuthal angular dependences, therefore it is possible to simultaneously determine all three terms by studying the angular dependence.

The HERMES collaboration carried out the first measurement of Collins and Sivers asymmetries [21] with electron and positron beams on a transversely polarized proton target. The COMPASS collaboration performed measurements with a muon beam on transversely polarized proton [22] and deuteron targets [23]. In Hall A at Jefferson Laboratory (JLab), an exploratory experiment E06-010 [24,25] was carried out, for the first time using an electron beam on a transversely polarized ^{3}He target. The extracted Collins and Sivers asymmetries were published [24]. In extracting these asymmetries, the pretzelosity term was not included. Its uncertainty was estimated and included in the systematic uncertainties.

II. EXPERIMENT

In this paper, we present the results of the pretzelosity asymmetry extracted from the JLab E06-010 data. As shown in Fig. 1, a 5.9-GeV electron beam was incident on a transversely polarized gaseous ^{3}He target with an average current of 12 μA. The target [26] was polarized by a spin-exchange optical pumping [27] of a Rb/K mixture, with which an average polarization is $55.4 \pm 2.8\%$. The scattered electrons were detected using the BigBite spectrometer [26] at beam right with a solid-angle acceptance of $\sim$64 msr. Three sets of

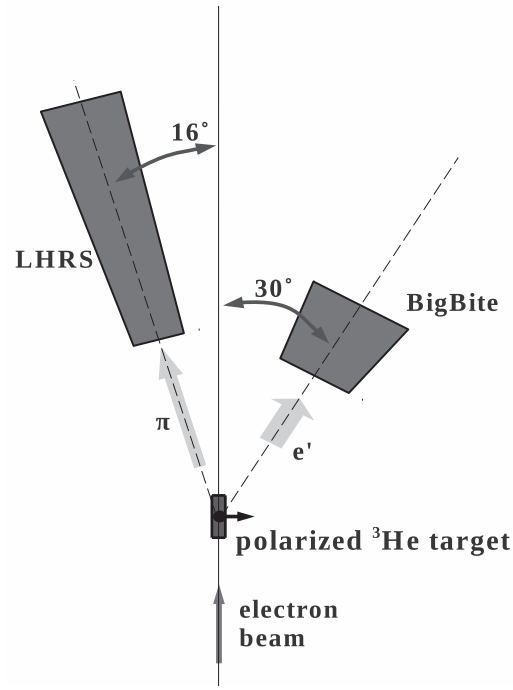

FIG. 1. The schematic view of the experiment E06-010.

drift chambers with 18 wire planes in total were used for tracking. Lead-glass preshower and shower detectors were used to identify electrons. The hadron contamination of the electron sample in the SIDIS process was suppressed to below 2% in the momentum range of 0.6–2.5 GeV. The produced hadrons were detected in the left arm of the high resolution spectrometers [26] (LHRS). A gas Cherenkov detector and two layers of lead-glass detectors provided a clean separation of pions from electrons. An aerogel Cherenkov detector and the coincident time-of-flight technique (about 25 m from the target to the LHRS focal plane) were employed to distinguish pions from kaons and protons.

To extract moments of the SSA, it is important to have the azimuthal angular coverage as complete as possible. In the case of pretzelosity asymmetry, the azimuthal angle is $(3\phi_h - \phi_s)$ and the range is $[0,2\pi]$. In the experiment, the BigBite and the LHRS spectrometer covered only part of the 2π angular range. To increase the angular coverage, four different target spin orientations orthogonal to the beam direction, transverse left, transverse right, vertical up, and vertical down, were used. For each target spin orientation the spectrometers covered only a section of the phase space as shown in the left panel of Fig. 2 (target spin vertical up). However, data from all four orientations, when combined, covered the full angular range as shown in the right panel of Fig. 2, where magenta, green, red, and blue are for horizontal beam left, horizontal beam right, vertical up, and vertical down, respectively. In order to achieve target polarizations in these four orientations, three pairs of mutually orthogonal Helmholtz coils were employed. During the experiment, the target spin direction was flipped every 20 min using the adiabatic fast passage technique, in which the magnetic holding field direction and strength remained unchanged.

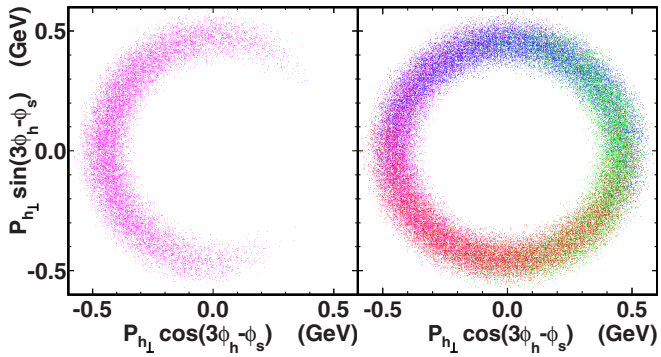

FIG. 2. (Color online) The coverage of the lowest-x-bin data in the phase space defined as $(P_{h\perp},3\phi_h-\phi_s)$ in a polar coordinate. In each panel the x axis is defined as $P_{h\perp}\cos(3\phi_h-\phi_s)$ and the y axis is defined as $P_{h\perp}\sin(3\phi_h-\phi_s)$. The left panel shows the data in only one target spin orientation (horizontal beam left), while the right panel shows the data in all four orientations.

III. DATA ANALYSIS

Several kinematic cuts were used to select SIDIS events: the negative square of the four-momentum transfer $Q^2 > 1\ \mathrm{GeV}^2$, the invariant mass of the virtual photon-nucleon system $W > 2.3$ GeV, and the invariant mass of the undetected final state particles $W' > 1.6$ GeV. Data were divided into four Björken-x bins with roughly equal statistics. The central kinematics are presented in Table I. To minimize the systematic uncertainties, the data taken between each of two flips of the target spin were divided into two sections. Two adjacent data sets with opposite spin directions formed a local pair, from which a local raw asymmetry was extracted. Throughout the experiment, approximately 2850 of such local raw asymmetries were combined to form the total raw asymmetry. Pretzelosity moments were extracted by a least-χ^2 fit of the total raw asymmetry to Eq. (1), in a two-dimensional (ϕ_h,ϕ_s) histogram which contained 100 bins in the 2π range for each quantity.

In the polarized ^{3}He target, a small amount ($\sim$1% in volume) of N_2 gas was mixed with ^{3}He gas to reduce depolarization effects. The nitrogen nuclei also contributed to the total measured yield and thus diluted the raw asymmetries. To obtain the asymmetries on ^{3}He, a correction for the nitrogen dilution was applied to the raw asymmetries, as shown in Eq. (2):

$$A^p_{^3\mathrm{He}} = A^p_{\mathrm{raw}} \Big/ \left(1 - \frac{N_{\mathrm{N}_2}\sigma_{\mathrm{N}_2}}{N_{\mathrm{N}_2}\sigma_{\mathrm{N}_2} + N_{^3\mathrm{He}}\sigma_{^3\mathrm{He}}}\right). \qquad (2)$$

In Eq. (2) the σ's are the unpolarized cross sections and the N's are the number densities. In the experiment, the cross section ratio $\sigma_{^3\mathrm{He}}/\sigma_{\mathrm{N}_2}$ was measured through dedicated data taking with a reference target cell filled with a known amount of ^{3}He and N_2 gases. The number densities of ^{3}He and N_2 in the polarized target were verified by taking the data of electron elastic scattering on both the reference target and the production ^{3}He target [28]. Another important correction was made due to the pair-produced background electrons (and positions) in the SIDIS electron samples. This is especially significant in the lowest x bin corresponding to the lowest momentum. Dedicated data were taken with the BigBite spectrometer in reversed polarity to measure the yield of the coincident $(e,e^+\pi^\pm)$ events, which is identical to the yield of $(e,e'\pi^\pm)$ events in the charge-symmetric pair production. This effect was corrected as a dilution since the measured asymmetries of the coincident $(e,e^+\pi^\pm)$ events were consistent with zero.

In the analysis, the systematic uncertainties due to omission of the other ϕ_h- and ϕ_s-dependent terms in the binned least-χ^2 fit, including the Cahn ($\langle\cos(\phi_h)\rangle$) and Boer-Mulders ($\langle\cos(2\phi_h)\rangle$) effects, higher-twist terms ($\langle\sin(\phi_s)\rangle$ and $\langle\sin(2\phi_h-\phi_s)\rangle$), and the A_{UL} terms ($\langle\sin(\phi_h)\rangle$ and $\langle\sin(2\phi_h)\rangle$) [20,29] were estimated. The A_{UL} terms were induced by a small longitudinal component of the target polarization in the virtual photon-nucleon center-of-mass frame of the SIDIS process. Of all these effects, the uncertainty of the $\langle\sin(2\phi_h-\phi_s)\rangle$ term was largest ($\sim$16% of the statistical uncertainty), followed by the $\langle\sin(\phi_s)\rangle$ term ($\sim$14% of the statistical uncertainty). To estimate the systematic uncertainty induced by $K^\pm$ contamination in the $\pi^\pm$ example, the coincident $(e,e'K^\pm)$ events were selected and the $\sin(3\phi_h-\phi_s)$ term of the asymmetry was extracted by maximum likelihood method. Then, the systematic uncertainty was evaluated as the difference between the $\sin(3\phi_h-\phi_s)$ terms of the $(e,e'\pi^\pm)$ and the $(e,e'K^\pm)$ samples, weighted by the contamination ratios of the $K^\pm$ in $\pi^\pm$ samples. Other ingredients of the systematic uncertainties included the yield drift, the target polarization, the target-density fluctuation, the detector tracking efficiency, the DAQ live time, the nitrogen dilution, and the photon contamination in the BigBite spectrometer. Since those ingredients have no azimuthal angular dependence and share the same data set of [24], they have the same values as in [24].

TABLE I. Central kinematics for the four x bins. The Björken scaling variable x, the fractional e^- energy loss y, the hadron energy fraction z with respect of electron energy transfer in the target rest frame, and the transverse momentum $P_{h\perp}$ are all defined following the notation in Ref. [19].

x	Q^2 GeV^2	y	z	$P_{h\perp}$ GeV	W GeV	W' GeV
0.156	1.38	0.81	0.50	0.44	2.91	2.07
0.206	1.76	0.78	0.52	0.38	2.77	1.97
0.265	2.16	0.75	0.54	0.32	2.63	1.84
0.349	2.68	0.70	0.58	0.24	2.43	1.68

IV. RESULTS

The extracted moments of the pretzelosity asymmetry on the ^{3}He target are shown in the top two panels of Fig. 3 and in Table II. Only statistical uncertainties are included in the error bars. The experimental systematic uncertainties are combined in quadrature and shown as the band labeled as "sys." All the extracted π^+ and π^- pretzelosity terms, which were cross checked with an unbinned maximum-likelihood fit, are small and consistent with zero within the uncertainties. This observation further supports the assumption in previous

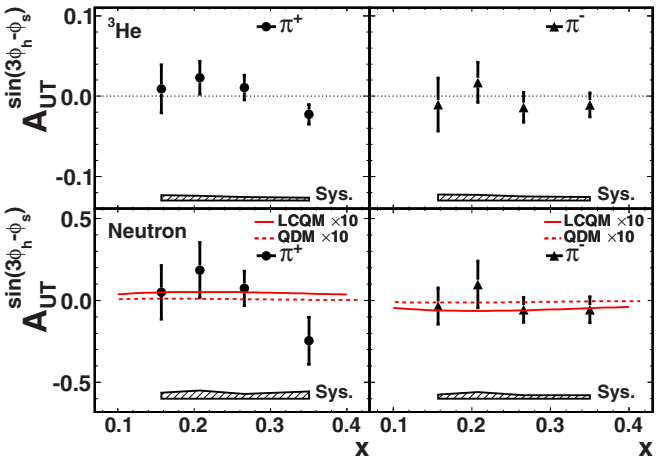

FIG. 3. (Color online) The extracted pretzelosity asymmetries on ^{3}He nuclei (top panels) and on the neutron (bottom panels) are shown together with uncertainty bands for both π^+ and π^- electron-production.

analysis [24] that the inclusion of the pretzelosity term has little effect on the extraction of the Collins and Sivers term.

To extract the pretzelosity asymmetries on neutron, the effective polarization method was used:

$$A_n^p = \frac{1}{(1-f_p)P_n}\left(A_{^3\mathrm{He}}^p - f_p A_p^p P_p\right), \tag{3}$$

where the proton dilution factor $f_p \equiv 2\sigma_p/\sigma_{^3\mathrm{He}}$ was obtained by measuring the yields of unpolarized proton and ^{3}He targets at the same kinematics. The same model uncertainty due to final-state interactions as in [24] was taken into account for f_p. $P_n = 0.86^{+0.036}_{-0.02}$ and $P_p = -0.028^{+0.009}_{-0.004}$ are the effective polarizations of the neutron and proton in a ^{3}He nucleus [30,31], respectively. Due to the scarcity of available data and the small effective polarization of the proton, no correction was applied to account for the effect due to the proton asymmetry. The uncertainty due to this omission was estimated and included in the systematic uncertainty. For positive pions at the highest x bin, the asymmetry is magnified by nearly one order of magnitude from ^{3}He to the neutron, due to the large proton dilution.

The extracted moments of the pretzelosity asymmetry on the neutron are listed in Table III and are also shown in the bottom two panels of Fig. 3, in which they are compared with the quark-diquark model (QDM) [16] and light-cone constituent-quark model (LCQM) [32,33] calculations. As in the two upper panels, the error bars shown only represent the statistical uncertainties, while the bands labeled "sys." represent the systematic uncertainties. Since both amplitudes of model predictions and differences between the two predictions are hardly visible compared to the statistical uncertainties, the curves in the two panels are multiplied by a factor of 10. The extracted neutron asymmetries of both $(e,e'\pi^+)$ and $(e,e'\pi^-)$ are again consistent with zero. Compared to the $\sin(\phi_h+\phi_s)$ terms, the $\sin(3\phi_h-\phi_s)$ terms are suppressed due to the different azimuthal dependent terms besides the TMDs and the Collins fragmentation functions in the convolution [20]. As suggested in [16], a large $P_{h\perp}$ coverage such as that planned for future experiments [34] with a higher statistical precision, is necessary to observe nonzero pretzelosity asymmetry. It is worth mentioning that the small value for the asymmetry predicted by the quark-diquark model (of the order of 10^{-3}) is mainly due to kinematic suppression and hence does not necessarily imply that $h_{1T}^{\perp}$ is small. In this calculation, $h_{1T}^{\perp}$ is proportional to the OAM of the quarks, originating from a Melosh rotation of the quark spin distribution between the instant and the light-cone frame.

TABLE II. Values and uncertainties of the extracted ^{3}He asymmetries.

x	π^+ terms			π^- terms		
	asym.	stat.	sys.	asym.	stat.	sys.
0.156	0.009	0.030	0.007	−0.010	0.033	0.007
0.206	0.023	0.020	0.006	0.017	0.025	0.007
0.265	0.011	0.015	0.004	−0.014	0.019	0.005
0.349	−0.023	0.012	0.004	−0.011	0.015	0.004

TABLE III. Values and uncertainties of the extracted neutron asymmetries.

x	π^+ terms			π^- terms		
	asym.	stat.	sys.	asym.	stat.	sys.
0.156	0.049	0.164	0.038	−0.035	0.110	0.025
0.206	0.185	0.169	0.050	0.097	0.143	0.040
0.265	0.074	0.105	0.030	−0.057	0.076	0.022
0.349	−0.246	0.143	0.044	−0.057	0.079	0.022

V. CONCLUSION

In summary, we present the first measurement of pretzelosity asymmetries on a transversely polarized ^{3}He target, utilizing charged pion production in the semi-inclusive deep-inelastic scattering. The asymmetries are consistent with zero within experimental uncertainties, and are also consistent with model expectations. This work demonstrated an experimental approach for studying the $h_{1T}^{\perp}$ TMD and laid a foundation for future high-precision measurements [34].

ACKNOWLEDGMENTS

We acknowledge the outstanding support of the JLab Hall A staff and Accelerator Division in accomplishing this experiment. This work was supported in part by the U.S. National Science Foundation, and by U.S. DOE contract no. DE-AC05-06OR23177, under which Jefferson Science Associates, LLC operates the Thomas Jefferson National Accelerator Facility. This work was also supported by the National Natural Science Foundation of China under Grant Nos. 11135002 and 11120101004.

[1] J. Ashman *et al.* (European Muon Collaboration), Phys. Lett. B **206**, 364 (1988).
[2] S. E. Kuhn, J.-P. Chen, and E. Leader, Prog. Part. Nucl. Phys. **63**, 1 (2009).
[3] C. A. Aidala, S. D. Bass, D. Hasch, and G. K. Mallot, Rev. Mod. Phys. **85**, 655 (2013).
[4] A. Adare *et al.* (PHENIX Collaboration), Phys. Rev. D **84**, 012006 (2011).
[5] A. Adare *et al.* (PHENIX Collaboration), Phys. Rev. D **86**, 092006 (2012).
[6] D. de Florian, R. Sassot, M. Stratmann, and W. Vogelsang, Prog. Part. Nucl. Phys. **67**, 251 (2012).
[7] M. Guidal, H. Moutarde, and M. Vanderhaeghen, Rep. Prog. Phys. **76**, 066202 (2013).
[8] M. Anselmino, M. Boglione, U. D'Alesio, E. Leader, S. Melis, and F. Murgia, Phys. Rev. D **73**, 014020 (2006).
[9] V. Barone, F. Bradamante, and A. Martin, Prog. Part. Nucl. Phys. **65**, 267 (2010).
[10] G. A. Miller, Phys. Rev. C **68**, 022201 (2003).
[11] G. A. Miller, Phys. Rev. C **76**, 065209 (2007).
[12] H. Avakian, A. V. Efremov, P. Schweitzer, and F. Yuan, Phys. Rev. D **78**, 114024 (2008).
[13] H. Avakian, A. V. Efremov, P. Schweitzer, and F. Yuan, Phys. Rev. D **81**, 074035 (2010).
[14] C. Lorce' and B. Pasquini, Phys. Lett. B **710**, 486 (2011).
[15] M. Burkardt, arXiv:0709.2966 (2007).
[16] J. She, J. Zhu, and B.-Q. Ma, Phys. Rev. D **79**, 054008 (2009).
[17] J. Collins, Nucl. Phys. B **396**, 161 (1993).
[18] F. Yuan and J. Zhou, Phys. Rev. Lett. **103**, 052001 (2009).
[19] A. Bacchetta, U. D'Alesio, M. Diehl, and C. A. Miller, Phys. Rev. D **70**, 117504 (2004).
[20] M. Anselmino, M. Boglione, U. D'Alesio, S. Melis, F. Murgia, E. R. Nocera, and A. Prokudin, Phys. Rev. D **83**, 114019 (2011).
[21] A. Airapetian *et al.* (HERMES Collaboration), Phys. Rev. Lett. **94**, 012002 (2005).
[22] M. Alekseev *et al.* (COMPASS Collaboration), Phys. Lett. B **692**, 240 (2010).
[23] M. Alekseev *et al.* (COMPASS Collaboration), Phys. Lett. B **673**, 127 (2010).
[24] X. Qian *et al.*, Phys. Rev. Lett. **107**, 072003 (2011).
[25] J. Huang *et al.*, Phys. Rev. Lett. **108**, 052001 (2012).
[26] J. Alcorn *et al.*, Nucl. Instrum. Methods Phys. Res. A **522**, 294 (2004).
[27] T. G. Walker and W. Happer, Rev. Mod. Phys. **69**, 629 (1997).
[28] Y. Zhang, X. Qian, and B.-T. Hu, Chinese Phys. C **36**, 610 (2012).
[29] A. Bacchetta *et al.*, J. High Energy Phys. 02 (2007) 093.
[30] X. Zheng *et al.*, Phys. Rev. C **70**, 065207 (2004).
[31] J. J. Ethier and W. Melnitchouk, Phys. Rev. C **88**, 054001 (2013).
[32] B. Pasquini, S. Cazzaniga, and S. Boffi, Phys. Rev. D **78**, 034025 (2008).
[33] S. Boffi, A. V. Efremov, B. Pasquini, and P. Schweitzer, Phys. Rev. D **79**, 094012 (2009).
[34] H. Gao *et al.*, Eur. Phys. J. Plus **126**, 2 (2011); JLab Proposal Report Nos. E12-10-006 and E12-11-108
[35] B.-Q. Ma and I. Schmidt, Phys. Rev. D **58**, 096008 (1998).